AFRL-ML-WP-TP-2007-458

MEASURES OF BULK AND GRAIN STRAIN IN DEFORMATION PROCESSES (PREPRINT)

Craig S. Hartley and Jonathan E. Spowart

APRIL 2007

Approved for public release; distribution unlimited.

STINFO COPY

MATERIALS AND MANUFACTURING DIRECTORATE
AIR FORCE RESEARCH LABORATORY
AIR FORCE MATERIEL COMMAND
WRIGHT-PATTERSON AIR FORCE BASE, OH 45433-7750

REPORT DOCUMENTATION PAGE

Form Approved
OMB No. 0704-0188

1. REPORT DATE *(DD-MM-YY)*	2. REPORT TYPE	3. DATES COVERED *(From - To)*
April 2007	Journal Article Preprint	

4. TITLE AND SUBTITLE
MEASURES OF BULK AND GRAIN STRAIN IN DEFORMATION PROCESSES (PREPRINT)

5a. CONTRACT NUMBER
In-house

5b. GRANT NUMBER

5c. PROGRAM ELEMENT NUMBER
62102F

6. AUTHOR(S)
Craig S. Hartley (El Arroyo Enterprises)
Jonathan E. Spowart (AFRL/MLLMD)

5d. PROJECT NUMBER
4347

5e. TASK NUMBER
RG

5f. WORK UNIT NUMBER
M02R4000

7. PERFORMING ORGANIZATION NAME(S) AND ADDRESS(ES)
El Arroyo Enterprises
231 Arroyo Sienna Drive
Sedona, AZ 86336

Metals Branch/Metals Development Team (AFRL/MLLMD)
Metals, Ceramics & Nondestructive Evaluation Division
Materials and Manufacturing Directorate
Air Force Research Laboratory, Air Force Materiel Command
Wright-Patterson Air Force Base, OH 45433-7750

8. PERFORMING ORGANIZATION REPORT NUMBER
AFRL-ML-WP-TP-2007-458

9. SPONSORING/MONITORING AGENCY NAME(S) AND ADDRESS(ES)
Materials and Manufacturing Directorate
Air Force Research Laboratory
Air Force Materiel Command
Wright-Patterson AFB, OH 45433-7750

10. SPONSORING/MONITORING AGENCY ACRONYM(S)
AFRL-ML-WP

11. SPONSORING/MONITORING AGENCY REPORT NUMBER(S)
AFRL-ML-WP-TP-2007-458

12. DISTRIBUTION/AVAILABILITY STATEMENT
Approved for public release; distribution unlimited.

13. SUPPLEMENTARY NOTES
Journal article submitted to International Journal of Plasticity. This paper contains color content.
The U.S. Government is joint author of this work and has the right to use, modify, reproduce, release, perform, display, or disclose the work. PAO Case Number: AFRL/WS 07-1032, 25 Apr 2007.

14. ABSTRACT
Many instances of severe plastic deformation produce a heterogeneous distribution of strain through a material. Common methods of describing the severity of deformation based on changes in the external dimensions of a specimen masks this heterogeneity, which is difficult to measure directly. This study describes a method of measuring internal strain based on the observation that networks of internal boundaries within a polycrystalline material deform locally in a manner congruent with the local metal flow. Appropriate measurements of the development of the spatial anisotropy of such networks with increasing deformation provide a basis for defining several measures of the local total strain. These quantities, called "grain strains" when the boundaries observed are grain boundaries, can serve as an experimental measure of the internal total strain in various locations in a specimen for comparison with computations based on finite element models using various constitutive relations.

15. SUBJECT TERMS
Grain Boundaries, Finite Strain, Optical Microscopy

16. SECURITY CLASSIFICATION OF:			17. LIMITATION OF ABSTRACT:	18. NUMBER OF PAGES	19a. NAME OF RESPONSIBLE PERSON (Monitor)
a. REPORT	b. ABSTRACT	c. THIS PAGE			Jonathan E. Spowart
Unclassified	Unclassified	Unclassified	SAR	42	19b. TELEPHONE NUMBER *(Include Area Code)* N/A

Standard Form 298 (Rev. 8-98)
Prescribed by ANSI Std. Z39-18

Measures of Bulk and Grain Strain in Deformation Processes

Craig S. Hartley[a] and Jonathan E. Spowart[b]

[a]*El Arroyo Enterprises, 231 Arroyo Sienna Drive, Sedona, AZ 86336*

[b]*Air Force Materials Laboratory, Materials and Manufacturing Directorate, Wright-Patterson AFB, OH 45433*

Abstract

Many instances of severe plastic deformation produce a heterogeneous distribution of strain through a material. Common methods of describing the severity of deformation based on changes in the external dimensions of a specimen masks this heterogeneity, which is difficult to measure directly. This study describes a method of measuring internal strain based on the observation that networks of internal boundaries within a polycrystalline material deform locally in a manner congruent with the local metal flow. Appropriate measurements of the development of the spatial anisotropy of such networks with increasing deformation provide a basis for defining several measures of the local total strain. These quantities, called "grain strains" when the boundaries observed are grain boundaries, can serve as an experimental measure of the internal total strain at various locations in a specimen for comparison with computations based on finite element models using various constitutive relations. Experimental measurements of the grain strains at the center of ferritic steel sheet rolled in nominally 10% increments to 50% total reduction in thickness illustrate the method and correlate well with corresponding strains based on measures of the change in thickness of the sheet and the assumption of plane strain.

Keywords: A. Grain Boundaries; B. Finite Strain; C. Optical Microscopy

---

1. Background

Typical measures of the degree of deformation in a severe plastic deformation operation employ a single number derived from the change some conveniently measured external dimension of a specimen before and after deformation. Such measures imply uniform and homogeneous deformation throughout the deforming region, an assumption known not to be satisfied even for the simplest processes. Measures of the heterogeneity of deformation during such operations are necessarily destructive because of our inability to observe changes in the interior of the workpiece. Consequently the development of strain must be determined from destructive measurements made on specimens examined after successive increments of deformation.

Two methods employed for this purpose are Physical Modeling (Aoyagi and Ohta, 1983; Piwnik, 1986), a simulation of the deformation process using a plasticine workpiece, and Visioplasticity (Shabaik and Thomsen, 1973). The latter technique employs initial billets of actual metallic workpiece materials that are sectioned prior to deformation, imprinted with a grid on the exposed section plane and reassembled before processing. The workpiece is removed from the tooling before it has been completely deformed and sectioned to reveal the deformed grid. Measurements of the undeformed and deformed grids provide a basis for the computation of local measures of deformation.

Early studies of the development of microstructural anisotropy in rolled mild steel sheet by Hartley and Dehghani (1987) established that the principal axes of the Fabric Tensor characterizing microstructural anisotropy were parallel to the principal directions of deformation during rolling. Also, the principal values of a second rank tensor describing the spatial anisotropy of L(**t**), the mean linear intercept of test lines with grain ferrite boundaries along a direction parallel to the unit vector, **t**, changed proportionately to the change in dimensions of the rolled sheet along the rolling, transverse and thickness directions. Recently, Hartley (2006) demonstrated that a measure of finite internal strain called grain strain can be defined based on the dimensions of the representation quadric of the spatial variation L(**t**) with **t**. The values of grain strain obtained from a quantitative analysis of the grain boundary network in the deforming region of a tensile specimen were found proportional to, but not equal to, corresponding measures of the bulk external strain. The lack of coincidence of these measures was attributed to the non-uniformity of deformation throughout the deforming region.

In the following sections describe various finite strain measures based on homogeneous deformation of the bulk material and local deformation of microstructures that can be described by weak anisotropy[*]. Next, these measures are employed to analyze the development of total deformation at the midplane of a rolled iron sheet and are compared with comparable measures of finite bulk strain. The final section discusses the relative

[*] *Kanatani (1984) defines weak anisotropy as that for which, $P_L(\mathbf{t})$, the spatial variation of the mean linear intercept of grain boundaries with a test line parallel to the unit vector, **t**, is quadratic in **t**.*

merits of various measures of finite strain in this context and the difference between these measures and conventional measures of bulk strain. An application of the measurement to the verification of calculations employing various constitutive equations to model finite deformation is proposed.

2. Finite Bulk Strain Measures

The definitions of bulk strain[†] tensors applicable to a deformation process are based on stretch ratios calculated from changes in the external dimensions of a workpiece, assuming constant volume and any other geometric constraints applicable to the process. For example, a state of plane strain with no change in the width or long transverse dimension approximates the deformation of a sheet subjected to reduction in thickness by rolling. Then a billet with initial length, width and thickness, l_o, w_o and t_o, respectively, isochorically deformed by rolling along the length direction to reduce the thickness to the final dimensions l, w and t obeys the relationship

$$l_o w_o t_o = lwt \tag{1}$$

with $w_o = w$. Since no rotation occurs globally, the rotation matrix in the polar decomposition of the deformation gradient is the identity matrix, $\mathbf{R} = \mathbf{I}$, leading to the result that the right and left stretch tensors, **U** and **V**, are equal, as are the right and left Cauchy-

[†] *In the following discussion, strain refers to total strain, which for large deformations is, to a good approximation, equal to the plastic strain.*

Green tensors, **C** and **B**. The stretch ratios in the principal directions of bulk deformation are

$$\Lambda_\ell = \frac{\ell}{\ell_o}, \Lambda_w = 1 \text{ and } \Lambda_t = \frac{t}{t_o} = \frac{1}{\Lambda_\ell}. \tag{2}$$

Comparison with conventional measures of deformation by rolling is facilitated by noting that $t = t_o - \Delta t$, so $\Lambda_t = [1 - \Delta t/t_o]$, where the second term in brackets is the fractional reduction in thickness due to rolling. Equation (2) permits all principal stretch ratios to be expressed in terms of this quantity. For the deformation considered, the right stretch tensor, **U**, becomes

$$\mathbf{U} = \begin{bmatrix} \Lambda_t^{-1} & 0 & 0 \\ 0 & 1 & 0 \\ 0 & 0 & \Lambda_t \end{bmatrix} \tag{3}$$

from which $\mathbf{C} = \mathbf{U}^2$ provides the necessary information for calculation of various strain tensors (Malvern, 1969). Equation (3) is referred to the principal axes of deformation parallel to the rolling (ℓ), long transverse (w) and short transverse (t) directions. In the following discussion all tensors will be expressed in this coordinate system.

The logarithmic strain, $\mathbf{E}_{\ell n}$, also called true or natural strain, is a common measure of finite deformation produced by processes involving simple geometrical shapes of the workpiece. The tensor form of $\mathbf{E}_{\ell n}$ is defined in terms of the right stretch tensor as (Lubliner, 1990)

$$\mathbf{E}_{\ell n} = \ln(\mathbf{U}). \tag{4}$$

For the example of rolling described above the tensor takes the form

$$\mathbf{E}_{\ell n} = \begin{bmatrix} -\ell n\left(\Lambda_t\right) & 0 & 0 \\ 0 & 0 & 0 \\ 0 & 0 & \ell n\left(\Lambda_t\right) \end{bmatrix} \tag{5}$$

in terms of the stretch ratio in the thickness direction, Λ_t. This strain measure has the convenient feature that successive increments of strain are additive. In addition, the trace of $\mathbf{E}_{\ell n}$ vanishes identically for deformation of any magnitude at constant volume. The conventional strain, $\mathbf{E}_c$, is defined in terms of $\mathbf{U}$ as

$$\mathbf{E}_c = \mathbf{U} - \mathbf{I}\,. \tag{6}$$

For the rolling example

$$\mathbf{E}_c = \begin{bmatrix} \Lambda_t^{-1} - 1 & 0 & 0 \\ 0 & 0 & 0 \\ 0 & 0 & \Lambda_t - 1 \end{bmatrix} \tag{7}$$

referred to the same principal directions as $E_{\ell n}$.

Both Lagrangian and Eulerian forms of finite strain tensors are defined in terms of $\mathbf{C}$ (in this case), allowing for different choices of reference states. The Green-St. Venant (Lagrangian) Finite Strain tensor is (Malvern, 1969)

$$\mathbf{E} = \left(\frac{\mathbf{C} - \mathbf{I}}{2} \right), \tag{8}$$

which, for the case of plane strain, becomes

$$\mathbf{E} = \frac{1}{2}\begin{bmatrix} \Lambda_t^{-2} - 1 & 0 & 0 \\ 0 & 0 & 0 \\ 0 & 0 & \Lambda_t^2 - 1 \end{bmatrix}. \tag{9}$$

The Almansi (Eulerian) Finite Strain tensor is[‡]

$$\mathbf{E}^* = \left(\frac{\mathbf{I} - \mathbf{C}^{-1}}{2} \right), \tag{10}$$

whence

$$\mathbf{E}^* = \frac{1}{2}\begin{bmatrix} 1 - \Lambda_t^2 & 0 & 0 \\ 0 & 0 & 0 \\ 0 & 0 & 1 - \Lambda_t^{-2} \end{bmatrix}. \tag{11}$$

for rolling.

For some purposes it is useful to express the work of homogeneous deformation in a deformation process as the product of a single, scalar measure based on the state of strain at the end of the process and a similar measure of the flow stress of the material. The effective, or equivalent, strain, based on an analogous definition for incremental strain (Malvern, 1969), is such a quantity. For a particular strain tensor, $\mathbf{E}_s$, the effective strain is defined as

$$\overline{\varepsilon} = \sqrt{\frac{4\mathrm{II}_{\hat{\mathbf{E}}_s}}{3}}, \tag{12}$$

[‡] *Note that equations (10) and (11) apply in the present case only because the right and left Cauchy-Green tensors are equal due to the absence of bulk rotation.*

where $II_{\hat{\mathbf{E}}_s}$ is the second invariant of the deviatoric strain tensor at the end of the deformation process. This invariant can be written as

$$II_{\hat{\mathbf{E}}_s} = \frac{1}{2}\left[\mathbf{E}_s : \mathbf{E}_s - \left(\mathrm{Tr}\left(\mathbf{E}_s\right)\right)^2\right] \tag{13}$$

where $\mathrm{Tr}(\mathbf{E_s})$ is the trace of $\mathbf{E_s}$ and $\mathbf{E_s}:\mathbf{E_s} = \mathrm{Tr}(\mathbf{E_s}\cdot\mathbf{E_s})$ is the inner product of $\mathbf{E_s}$ with itself. The factor of 4/3 is chosen so that an isochoric, uniaxial tensile strain results in an effective strain equal to the tensile strain. The conjugate effective stress in this case is the uniaxial tensile stress. Based on equations (12) and (13), expressions for effective bulk strains can be written in terms of Λ_t using equations (5), (7), (9) and (11). For the particular case of bulk deformation examined in the present study, where the Right and Left Cauchy-Green tensors are equal, the equivalent strain is the same whether calculated from the Lagrangian or Eulerian finite strain tensor.

3. Finite Local Strain Measures Based on Networks of Internal Boundaries

Networks of inter- and intra-phase interfaces in polycrystalline alloys deformed by various deformation processes often develop symmetries based on those of the associated processes. The spatial variation of the mean intercept density, $P_L(\mathbf{t})$, the number of intersections per unit length of a test line parallel to the unit vector, **t**, with a selected class of internal boundaries, is a common measure of the anisotropy of such a network. The surface area per unit volume of these boundaries, S_V, depends on $\overline{P}_L$, the average value of $P_L(\mathbf{t})$ over all possible orientations of test lines, through the relationship

$$S_V = 2\overline{P}_L . \tag{14}$$

When the boundaries considered are grain boundaries $\overline{L} = \overline{P}_L^{-1}$, the mean distance between grain boundaries, is the global quantity commonly used to relate mechanical properties, such as yield stress, to the microstructure.

When deformation is anisotropic, the resulting internal boundary network also deforms anisotropically, which can influence subsequent mechanical behavior that depends on the orientation of internal boundaries relative to the applied principal stresses. Measurements of this anisotropy are based on a statistical counting process in which test lines having a total length, L, and lying parallel to a direction, **t**, with known orientation relative to a reference direction, are superimposed on a plane of observation. The number of intersections, N, of test lines with a selected class of boundaries in the section, divided by L gives $P_L(\mathbf{t})$ for that class of boundary.

A proper three-dimensional determination of $P_L(\mathbf{t})$ requires measurements on three non-coplanar sections intersecting in the same point. The value of $\overline{P}_L$ so determined is then assigned to the point in common to these sections. In practice this is not possible, since the destructive process of preparation of metallographic sections for each measurement makes it impossible to include comparable neighborhoods of the common point on the three planes of observation. In addition, the array of test lines employed defines a "gauge volume" for the measurement, having the point of intersection of planes of observation as its centroid. For a given statistical accuracy, the shape and size of this volume will vary with the extent of the anisotropy. Values of $P_L(\mathbf{t})$, S_V and $\overline{P}_L$ associated with the common

point can be considered field properties of the microstructure defined by the usual limiting process of considering them to be the limiting values of volume averages over successively small gauge volumes as the gauge volume approaches zero. These points will be discussed further in a later section.

Weak anisotropy as defined by Kanatani (1984) can be expressed

$$P_L(\mathbf{t}) = \frac{1}{L(\mathbf{t})} = \tilde{\mathbf{t}}\mathbf{M}\mathbf{t}, \tag{15}$$

where the tilde indicates the transpose of the column vector, **t**, and **M** is a symmetric, second rank tensor called the Microstructural Anisotropy Tensor (MAT) (Hartley, 2006). Since $\overline{P}_L$ is the average of $P_L(\mathbf{t})$ over all possible orientations of **t**,

$$\overline{P}_L = \frac{1}{4\pi}\int_{S_2}\left(\tilde{\mathbf{t}}\mathbf{M}\mathbf{t}\right)d\mathbf{n} = \frac{\mathrm{Tr}(\mathbf{M})}{3} \tag{16}$$

where S_2 is the set of all surface normals to the unit sphere, d**n** is the element of area on the surface of the unit sphere[§] and Tr(**M**) is the trace of **M**. For a completely isotropic network of internal boundaries

$$\mathbf{M} = \overline{P}_L\mathbf{I} \tag{17}$$

where **I** is the identity matrix. Thus the representation quadric for **M** is a sphere with radius $\frac{1}{\sqrt{\overline{P}_L}}$.

[§] *This notation for the element of surface area is employed to emphasize that the relationship is independent of coordinate system.*

To utilize an internal boundary network as an embedded grid for the purpose of measuring strain, consider a vector $\mathbf{x} = \mathbf{t}\,|L(\mathbf{t})|$ in the reference state deformed to an image, $\mathbf{x}' = \mathbf{t}'\,|L'(\mathbf{t}')|$, in the deformed state. In both cases an equation of the form of equation (15) gives the spatial dependence of the intercept density. Both **x** and **t** are related to their images in the deformed state by the deformation gradient, **F** (Malvern, 1969):

$$\mathbf{x}' = \mathbf{F}\mathbf{x} \text{ and } \mathbf{t}' = \mathbf{F}\mathbf{t}\,. \tag{18}$$

Substituting equation (16) into equation (15) and the corresponding expression for the deformed state gives the relationship

$$\mathbf{M} = \tilde{\mathbf{F}}\mathbf{M}'\mathbf{F} \tag{19}$$

relating the MATs in the reference and deformed states.

Multiplying equation (19) by the appropriate inverses gives

$$\tilde{\mathbf{F}}^{-1}\mathbf{M}\mathbf{F}^{-1} = \mathbf{M}'\,. \tag{20}$$

In the following definitions of strain, the reference state is chosen to be isotropic with a MAT of the form of equation (17), so that

$$\tilde{\mathbf{F}}^{-1}\mathbf{F}^{-1} = \left(\frac{3}{\mathrm{Tr}(\mathbf{M})}\right)\mathbf{M}'\,. \tag{21}$$

Equation (8) defines the Finger tensor, $\mathbf{B}^{-1}$, the inverse of the Left Cauchy-Green Tensor (Lubliner, 1990). The Right Cauchy-Green Tensor, **C**, is defined as

$$\mathbf{C} = \tilde{\mathbf{F}}\mathbf{F} \tag{22}$$

since $\mathbf{M}'$ is symmetric. Also, the choice of an isotropic reference state requires that the rotation matrix in the polar decomposition of **F** be **I**, so the deformations defined by this process are pure stretches. Then the right and left stretch tensors, **U** and **V**, respectively, are equal and

$$\mathbf{U} = \mathbf{V} = \sqrt{\mathbf{C}}\,. \tag{23}$$

During a deformation process we assume that changes in the network of internal boundaries occur primarily to accommodate changes in shape of the grains and/or phases that the boundaries enclose. Since these changes in shape are due primarily to shear processes occurring at essentially constant volume, measures of strain based on the change in shape of an internal boundary network refer to plastic strain, which, in the presence of relatively negligible elastic strain, is also the total strain. Consequently internal stresses cannot be calculated from such measures. The condition of constant volume requires that the determinant of the deformation gradient, $|\mathbf{F}|$, be unity (Malvern, 1969). Then by equation (21)

$$\left[\frac{\mathrm{Tr}(\mathbf{M})}{3}\right]^3 = |\mathbf{M}'| \tag{24}$$

for deformation at constant volume.

Using the above relationships, the conventional grain strain, $\mathbf{E}_e$, equation (6), becomes

$$\mathbf{E}_e = \sqrt{\frac{\mathrm{Tr}(\mathbf{M})\mathbf{M}'^{-1}}{3}} - \mathbf{I}\,, \tag{25}$$

and the Logarithmic grain strain, $\mathbf{E}_\ell$, equation (4) is

$$\mathbf{E}_{\ell} = \frac{1}{2}\left\{ \ell \mathrm{n}\left[\frac{\mathrm{Tr}(\mathbf{M})}{3} \right] + \ell \mathrm{n}\left(\mathbf{M}'^{-1} \right) \right\}. \tag{26}$$

Also by equation (8) the Green-St. Venant, or finite Lagrangian, grain strain tensor is

$$\mathbf{E} = \frac{1}{2}\left[\frac{\mathrm{Tr}(\mathbf{M})}{3} \mathbf{M}'^{-1} - \mathbf{I} \right] \tag{27}$$

for the network. The Almansi, or finite Eulerian, grain strain Tensor, equation (10), can be expressed as

$$\mathbf{E}^{*} = \frac{1}{2}\left[\mathbf{I} - \frac{3\mathbf{M}'}{\mathrm{Tr}(\mathbf{M})} \right] \tag{28}$$

since there is no rotation due to the choice of an isotropic reference state. In all cases for grain strains an effective grain strain can be calculated from the components of appropriate grain strain tensors using equation (12).

The choice of reference state is an important consideration in the calculation of strains defined by equations (28),(27) (25) and(26). For the Eulerian finite strain measure based on the deformation of a grain boundary network, Hartley (2006) proposed that the reference state for a deformed specimen be a hypothetical specimen having an isotropic network of grain boundaries with the same surface area per unit volume as the deformed specimen. This results in Tr(**M**) = Tr(**M**′), permitting the determination of relevant quantities to be made on the same specimen. It is also consistent with the use of the current state as a reference in the definition of Eulerian strain. This choice of reference state results in **E*** being completely deviatoric, as can easily be verified by direct substitution of the preceding relationship into equation (28).

The initial state is an alternative reference state, consistent with the Lagrangian definition of strain, equation (27). In this formulation the reference state is still isotropic, but the value of $\overline{P}_L$ is that for material in the undeformed state. In typical metal forming operations the starting material possesses some residual microstructural anisotropy characteristic of its thermo-mechanical history. Although this anisotropy generally has a different symmetry than that introduced by the subsequent processing operations, the value of $\overline{P}_L$ obtained from stereological measurements on the starting material is an invariant, hence it is the appropriate value to use in equation (17) for the MAT of the reference state. Also, in analyzing a deformation process in which the deformation is increased in successive increments of bulk strain, the initial value of $\overline{P}_L$ can be estimated by extrapolation to zero bulk strain the values of $\overline{P}_L$ for successive increments. This is the procedure employed for analysis of data in the present study. The initial condition is also the appropriate reference state for the conventional strain and the logarithmic strain, defined by equations (25) and (26), respectively. Values of effective grain strain can be calculated from the components of the grain strain tensors according to equation (12).

In the simplest model of large-scale plastic deformation, assuming that the number of grains per unit volume remains constant and deformation is homogeneous and uniform throughout the specimen, bulk strain and grain strain are equal (Hartley and Ünal, 1983; Hartley, 2006). However in practice deformation is never completely uniform and some fragmentation of grains occurs, leading to an increase in grain boundary area per unit

volume. These effects cause the grain strains measured at various points in the interior of a specimen to differ from those measured from changes in the exterior dimensions. Nevertheless, grain strains averaged across a cross-section of the specimen normal to a principal direction of deformation should equal the bulk strain in that direction. This study will not test this hypothesis.

4. Experimental Program

The grain boundary network images were obtained from optical digital micrographs of lightly-etched metallographic specimens, taken from rolled sheets of ultra-low (0.007 wt%) carbon steel. Five sets of images were obtained, one from each rolling condition, after actual rolling strains of 9.13%, 19.1%, 31.3%, 40.0%, and 48.7%. Each subsequent rolling condition thereby represents an additional 10% (nominal) reduction in thickness per pass from the as-received, 0.115"-thick hot-band rolled condition. Care was taken not to reverse the rolling direction on each subsequent pass. All rolling was carried out at room temperature, with a surface feed rate of 25 surface feet per minute.

Metallographic specimens were obtained from the centroids of the rolled sheets, with great care taken to maintain orientation of the prepared specimen surface within ± 1º of the global sheet directions. Fig. 1 illustrates how three mutually-perpendicular metallographic sections were prepared from each rolled specimen; (A) containing the Rolling Direction (RD) and Long Transverse (LT), or width, directions; (B) containing RD and Short Transverse (ST), or thickness, directions, and; (C) containing LT and ST directions.

Attention was paid in obtaining the three sections as close together as possible, to reduce the influence of a finite "gauge volume" on the results of the analyses.

[INSERT FIG. 1]

Fig. 1. Specimen Location and Coordinate System Employed for Metallographic Analysis

Figs. 2(a) - (f) show a representative set of micrographs for a rolling strain of 31.3%, both in the as-etched (a) – (c), and as-binarized (d) – (f) conditions. Note the significant anisotropy of the grains due to rolling.

[INSERT FIGS. 2 (a-f)]

Rapid determination of P_L was made possible by using a PASCAL-based computer code (*Auto-MAT.2D*) which runs within the NIH Image/Scion Image freeware image processing environment (Mullens, 2003). This code allows the user to input the total number of parallel test lines to be cast on a previously binarized (thresholded) digital image of a grain boundary network. The code then calculates the average number of grain boundary crossings per unit test line length within a circular window centered on the centroid of the image. The angle of the test lines (α) is then rotated at 1º intervals in the plane of the image until the entire grain boundary network is sampled; ($0 \leq \alpha \leq \pi$). It was found that an angular resolution of 1º was sufficient to ensure sufficient resolution of P_L (α) without oversampling.

5. Results

5.1. General

The following sections compare eigenvalues of the grain strain tensors computed using various definitions of strain with the corresponding bulk strain components calculated from

the reduction in thickness by rolling and assuming plane strain in the LT direction. Consequently, for all measures of strain the bulk strain component in the LT direction was zero. In all measures of grain strain, the eigenvector corresponding to the largest positive eigenvalue occurred within a few degrees of the RD, the eigenvector associated with the largest negative eigenvalue occurred similarly close to the ST direction and the remaining eigenvector was closely parallel to the LT direction, in agreement with earlier observations (Hartley and Dehghani, 1987; Hartley, 2006). Components of the grain strain tensors in the LT direction are, in general, not zero but are generally small in magnitude compared to the other two. These values are all plotted on the zero bulk strain ordinate to illustrate the range of values obtained.

As described earlier, the reference state for the Lagrangian, Conventional and Logarithmic measures of strain was a hypothetical isotropic structure with the same surface area per unit volume as the actual undeformed structure. Since data for this condition was not available, the surface area per unit volume calculated from measurements on the deformed specimens was determined from equations(14), (16) and (17) for each value of reduction in thickness. The linear extrapolation of these values, plotted against the logarithmic bulk strain in the rolling direction, to zero bulk strain provided a value for $\overline{P}_L$ in the initial, undeformed condition. Determinants of $\mathbf{M}'$ for the various deformed conditions were calculated and compared to $|\mathbf{M}| = [\mathrm{Tr}(\mathbf{M})/3]^3$ to ascertain whether the condition of constant volume was satisfied during deformation according to equation (24). Table 1 presents these values.

Table 1

Determinants of Microstructural Anisotropy Tensors

% Reduction in Thickness	$\|\mathbf{M}\| \times 10^3$
9.13	1.8
19.1	2.0
31.3	2.3
40.0	3.0
48.7	2.6

Fig. 3 shows the variation of $\overline{P}_L$ with the logarithmic bulk strain component in the RD.

[INSERT FIGURE 3]

Fig. 3. Mean linear intercept of Ferrite boundaries vs. Logarithmic Bulk Strain in the RD

The following sections present the relationships between bulk and grain strains for the various components of strain for the strain tensors discussed earlier.

5.2. Grain Strain Components and Bulk Strain Components

Fig. 4 shows components of the logarithmic grain strain tensor plotted against corresponding components of the bulk strain. In order to display results for all strain components in the same quadrant, Fig. 4 and subsequent similar graphs show the negative of the grain strain component in the ST direction plotted versus the negative of the bulk strain in the same direction and the negative of the grain strain component in the LT direction is plotted versus the bulk strain component in the RD.

[INSERT FIGURE 4]

Fig. 4. Components of Logarithmic Grain Strain vs. Logarithmic Bulk Strain

The lines represent linear, least-squares fits to the data for strain components in the indicated directions.

Fig. 5 presents the components of the Conventional Grain Strain tensor as functions of the corresponding components of the Conventional Bulk Strain tensor. As in the previous section all components are plotted in the positive quadrant, but it should be noted that the components of grain strain in the LT and ST directions and the bulk strain in the ST direction are negative.

[INSERT FIGURE 5]

Fig. 5. Conventional Grain Strain Components vs. Conventional Bulk Strain Components

Figs. 6 and 7 show the components of the Green-St. Venant (Lagrangian) and Almansi (Eulerian) finite grain strain tensors as functions of the corresponding components of the bulk strain tensors. As for the previous cases, the grain strain components in the ST and LT directions are negative and the negative of the bulk strain in the ST direction is plotted.

[INSERT FIGURES 6 AND 7]

Fig. 6. Lagrangian Grain Strain Components vs. Lagrangian Bulk Strain Components

Fig. 7. Eulerian Grain Strain Components vs. Eulerian Bulk Strain Components

From Figs. 4 – 7 it is evident that the assumption of plane strain is not quite satisfied for the grain strain measurements using any of the strain measures. Consequently it is useful to employ effective strain to compare the state of strain at the center of the rolled sheet. Fig. 8 illustrates this comparison using each of the four strain measures to calculate an effective strain.

[INSERT FIGURE 8]

Fig. 8. Effective Grain Strains vs. Effective Bulk Strains

It is apparent from Fig. 8 that all measures of effective strain provide a consistent correlation between grain and bulk strains regardless of the definition of strain employed. The linear relationship plotted in Fig. 8 is a composite result where the effective grain strain computed with all definitions is employed with all computations of effective bulk strain and fitted to a linear form. The slope of this expression is 0.316 and the intercept is -0.007.

6. Discussion

6.1. Estimate of Errors of Measurement Relative to Second Order Fit

There exist certain directions within the rolled specimens, i.e. parallel to RD, LT or ST, which are contained in exactly two of the three section planes used for the determination of P_L. For example, the ST direction is vertical in Fig 1(e), and horizontal in Fig 1 (f). With a vanishingly-small gauge volume, one would expect that the values of P_L calculated in these directions from both micrographs would be identical. The fact that there is a small but significant difference between the two values of P_L suggests a basis for a simple error analysis. The following simple treatment addresses the effect of the finite gauge volume on the results for $P_L(\theta, \phi)$.

First, the experimental $P_L(\theta, \phi)$ data obtained from each of the mutually-perpendicular section planes is combined, and a least-squares curve fit of the form of Eqn. (15) is applied, where $t_1 = \cos\phi$, $t_2 = \cos\theta \sin\phi$ and $t_3 = \sin\theta \sin\phi$ with x_1 parallel to RD, x_2 parallel to LT, and x_3 parallel to ST. Next, the absolute difference, ΔP_L, between the P_L values obtained on each of the two intersecting, perpendicular planes (P_L', P_L'') is obtained:

$$\Delta P_L = \left| P_L' - P_L'' \right| . \tag{29}$$

Finally, the relative error is ΔP_L divided by the value of the corresponding value of P_L given by the curve fit in the common direction of measurement, P_L^*, to wit:

$$\frac{\Delta P_L}{P_L^*} = \frac{\left| P_L' - P_L'' \right|}{P_L^*} . \tag{30}$$

The data show no observed systematic variation of the relative error with increasing rolling strain.

Values of $\Delta P_L / P_L^*$ measured in the ST direction (0.015) are much smaller than those measured in either the RD or LT directions (0.062 and 0.079, respectively.) Taking the arithmetic mean of these values gives an overall error of 0.052, or ~ 5%. This error corresponds to a minimum gauge volume of 8.0×10^6 μm^3, calculated from the size of the field of view on each mutually-perpendicular sectioning plane, i.e. 200μm × 200μm × 200μm. Although a quantitative relationship between the gauge volume and the expected error in P_L is not immediately forthcoming from this analysis, it is reasonable to expect that this error will diminish as the gauge volume is reduced. However, this reduction can only be practically accomplished up to the point where the number of internal boundaries sampled is still large enough for statistical significance of the intercept density. Further uncertainties in measurement arising when the strain gradient is large relative to the strain require the use of 3-D boundary intercept data obtained by manual or automated serial sectioning, tomography or similar experimental techniques to ascertain the size of sampled volume necessary to achieve a desired accuracy.

6.2. Association of the Measured Grain Strain with a Specific Point

The grain strains obtained by any of the definitions employed earlier apply to a point at the centroid of the effective gauge volume for the measurements. For the examples presented the experimental technique requires that measurements be made on three mutually perpendicular planes that do not contain a common point. Consequently it is necessary to assume that the gradients in microstructure are sufficiently small over the effective gauge volume that the measurements obtained on each plane also apply to a parallel plane passing through the centroid of the gauge volume. This point is illustrated in Fig. 9, which shows a schematic illustration of the locations of the planes of polish (faces of the cube) and the parallel planes, to which the measurements are assumed to apply, intersecting at the center of the cube. The ellipsoid inside the cube represents the quadratic surface $P_L(\mathbf{t})$ obtained from a least-squares fit to the measurements.

Any errors or inconsistencies arising from the assumption of negligible gradients in the microstructure over the cube defined by the planes of polish will be eliminated by measurements on a three dimensional data set obtained from serial sectioning or other similar technique. Such data can be obtained from reconstructions of parallel serial sections to reveal the three-dimensional character of grain boundaries and other internal interfaces in a sample. Points within the reconstructed volume can then be selected for strain measurements. Since the locations of internal interfaces are now quantitatively known from the reconstruction, it is possible to construct a set of test lines with arbitrary orientations passing through each point. For each point the strain would be determined from the three-

dimensional variation of the density of intercepts with internal interfaces by a random set of test lines passing through the point using the techniques described in this work.

6.3. Relationship Between Bulk and Grain Strains

The fact that the bulk and grain strains are not equal is due to the generally non-uniform state of strain in the interior of the deformed material. That is, basing a measurement of bulk strain on changes in the external dimensions of the material and applying this measure to a point in the interior assumes that the deformation occurs uniformly throughout the material. However, even deformation processes with simple geometries are known to result in non-uniform distributions of strain throughout the workpiece. Consequently the grain strain, which is a measure of the total strain at a point in the interior of the workpiece, should not be expected to be numerically equal to the bulk strain in general.

It is important to recognize that grain strain is a measure of local total strain; hence it is not suitable for computation of internal stresses, which result from strain of the crystal lattice. A complete description of the components of strain at a point requires that both the total strain and the lattice (or elastic) strain be measured at the same point. Then the strain components can be obtained by the familiar multiplicative decomposition due to Kröner (1960) and Lee and Liu (1965).

7. Conclusions

The network of grain boundaries in a single phase material provides a useful internal network for the determination of the internal total strain field (grain strain) in a deformed

crystalline material. For this purpose the reference state from which the strain is measured is a hypothetical, isotropic (equiaxed) boundary network having the same boundary surface area per unit volume as the deformed specimen. For deformation processes that involve congruent changes in shape from the initial state to the final state, the grain strain so measured is proportional to the bulk strain calculated from changes in the overall specimen dimensions. Three-dimensional states of bulk strain described by an effective bulk strain produce a proportional effective bulk strain within the interior of the material. These conclusions apply regardless of the type of strain definition employed.

The effective gauge volume for a grain strain measurement depends on the mean dimensions and anisotropy of grains. Some of the uncertainties introduced by making measurements on two-dimensional planes of polish that do not intersect in a common point can be significantly reduced or eliminated by the use of three-dimensional reconstructions of selected volumes of material obtained by serial sectioning or tomography.
Grain strain cannot be employed to determine internal stresses, but when measured simultaneously with lattice strain at the same point, it provides the necessary information for the decomposition of finite strain into plastic and elastic (lattice) components in the interior.

A major application area for the techniques developed in this study is the experimental determination of the internal total strain field throughout a deformed material for the purposes of comparison with corresponding strains calculated with finite element programs employing various physical and constitutive assumptions. Such experiments performed in

parallel with finite element studies of processes involving severe plastic deformation can lead to the development of improved constitutive models for material behavior and the formulation of finite element codes that more accurately reflect the behavior of real materials.

Acknowledgements

The authors wish to thank the Air Force Research Laboratory, Materials and Manufacturing Directorate for provision of facilities for the experimental research. The materials used in this study were generously supplied by Ms. Beth A. Kneuppel of AK Steel Corporation, Middletown, OH. Financial sponsorship was supplied by the Air Force Research Laboratory, through the Air Force Office of Scientific Research, which also provided research facilities for one of the authors (CSH). The authors also gratefully acknowledge stimulating discussions with Dr. Oana Cazacu of the University of Florida Graduate Engineering Research Center, Shalimar, FL.

References

Aoyagi, K and Ohta, K, 1983, Material Deformation, Rolling Load and Torque in a Three-Roll Planetary Mill, J. Jpn. Soc. Technol. Plast., 24, 1039-1047

Hartley, CS, 2006, Strain and the Quantitative Characterization of Anisotropic Microstructures, Met. and Mat. Trans. A, 37A, 3531-3539

Hartley, CS and Ünal, E., 1983, Bulk Strain and Grain Strain in Axisymmetric Deformation, Acta Metall., 31, 525-528

Hartley, CS and Dehghani, M, 1987, Evolution of Microstructure During Cold Rolling, *Proc. 7th ICSMA*, 1987, edited by H. McQueen, *et al*., Vol. 2., Pergamon Press, New York, NY, 959-964

Kanatani, K, 1984, Stereological determination of structural anisotropy, Int. J. Engng. Sci., 22**,** 531-546

Kröner, E, 1960, Allgemeine Kontinuumstheorie der Versetzungen und Eigenspannungen, Arch. Rational Mech. and Analysis, 4, 273 - 334

Lee, EH and Liu, DT, 1967, Finite-Strain Elastic-Plastic Theory with Application to Plane-Wave Analysis, J. Appl. Phys., 38, 19-27

Lubliner, J, 1990, Plasticity Theory, Macmillan Publishing Company, NY, 440.

Mullens, HM, 2003, Auto-Mat 2D: A Macro for Automatically Calculating the Microstructural Anisotropy Tensor, PASCAL Code, AFML/ML, Wright-Patterson AFB, OH

Malvern, LE, 1969, Introduction to the Mechanics of a Continuous Medium, First Edition, Prentice-Hall Publishing Company, Englewood Cliffs, NJ.

Piwnik, J, 1986, Modeling of the Influence of Voids on the Behaviour of a Material Plastically Deformed in Extrusion**.** Obrobka Plast., 25, 31-40

Shabaik, A and Thomsen, EG, 1973, Computer aided Visioplasticity solution of some deformation problems, Proc. International Symposium on Foundations of Plasticity, Warsaw, Poland, 30 Aug – 2 Sept, 1972, 177-199

Figure Captions

Fig. 1. Specimen Location and Coordinate System Employed for Metallographic Analysis

Fig. 2. Representative digital micrographs of ultra-low carbon steel sheet, rolled to 31.3% total reduction (3 passes);

(a) as-etched, RD – LT plane;

(b) as-binarized, RD – LT plane;

(c) as-etched, RD – ST plane;

(d) as-binarized, RD – ST plane;

(e) as-etched, LT – ST plane;

(f) as-binarized, LT – ST plane.

Fig. 3. Mean linear intercept of Ferrite boundaries vs. Logarithmic Bulk Strain in the RD

Fig. 4. Components of Logarithmic Grain Strain vs. Logarithmic Bulk Strain

Fig. 5. Conventional Grain Strain Components vs. Conventional Bulk Strain Components

Fig. 6. Lagrangian Grain Strain Components vs. Lagrangian Bulk Strain Components

Fig. 7. Eulerian Grain Strain Components vs. Eulerian Bulk Strain Components

Fig. 8. Effective Grain Strains vs. Effective Bulk Strains

Fig. 9. Schematic Illustration of Gauge Volume of Measurements

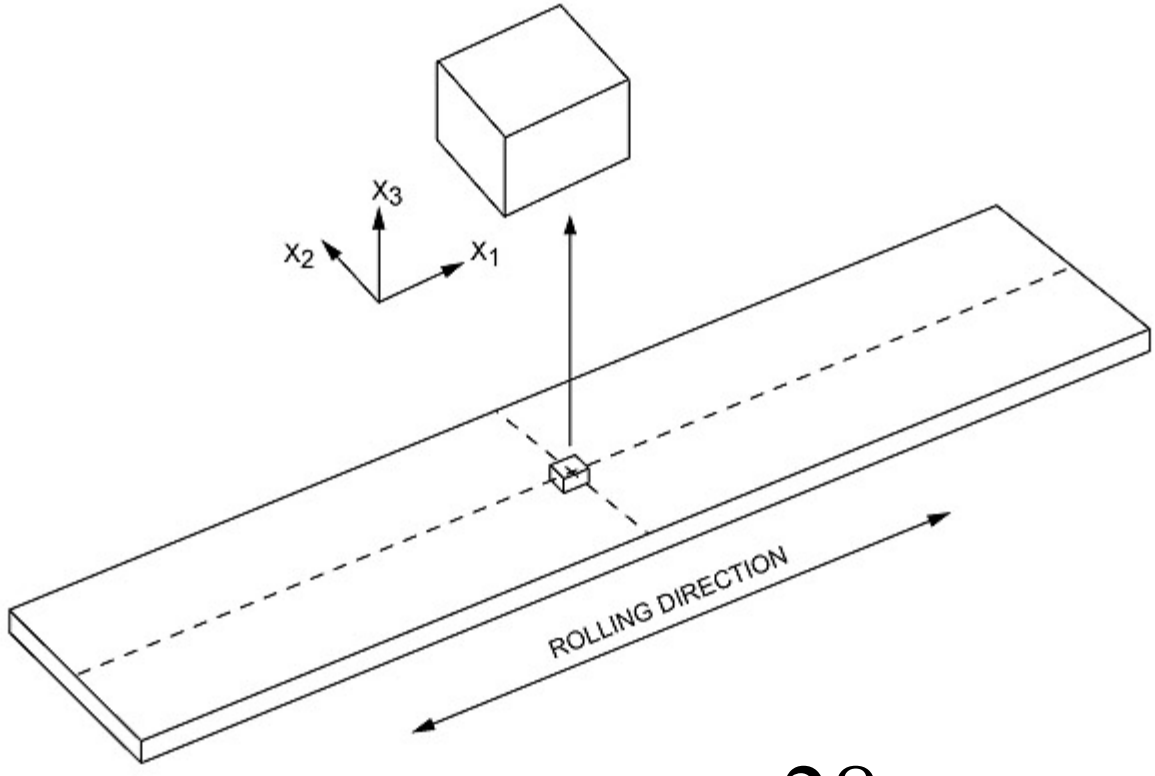
X3
X2
X1
ROLLING DIRECTION

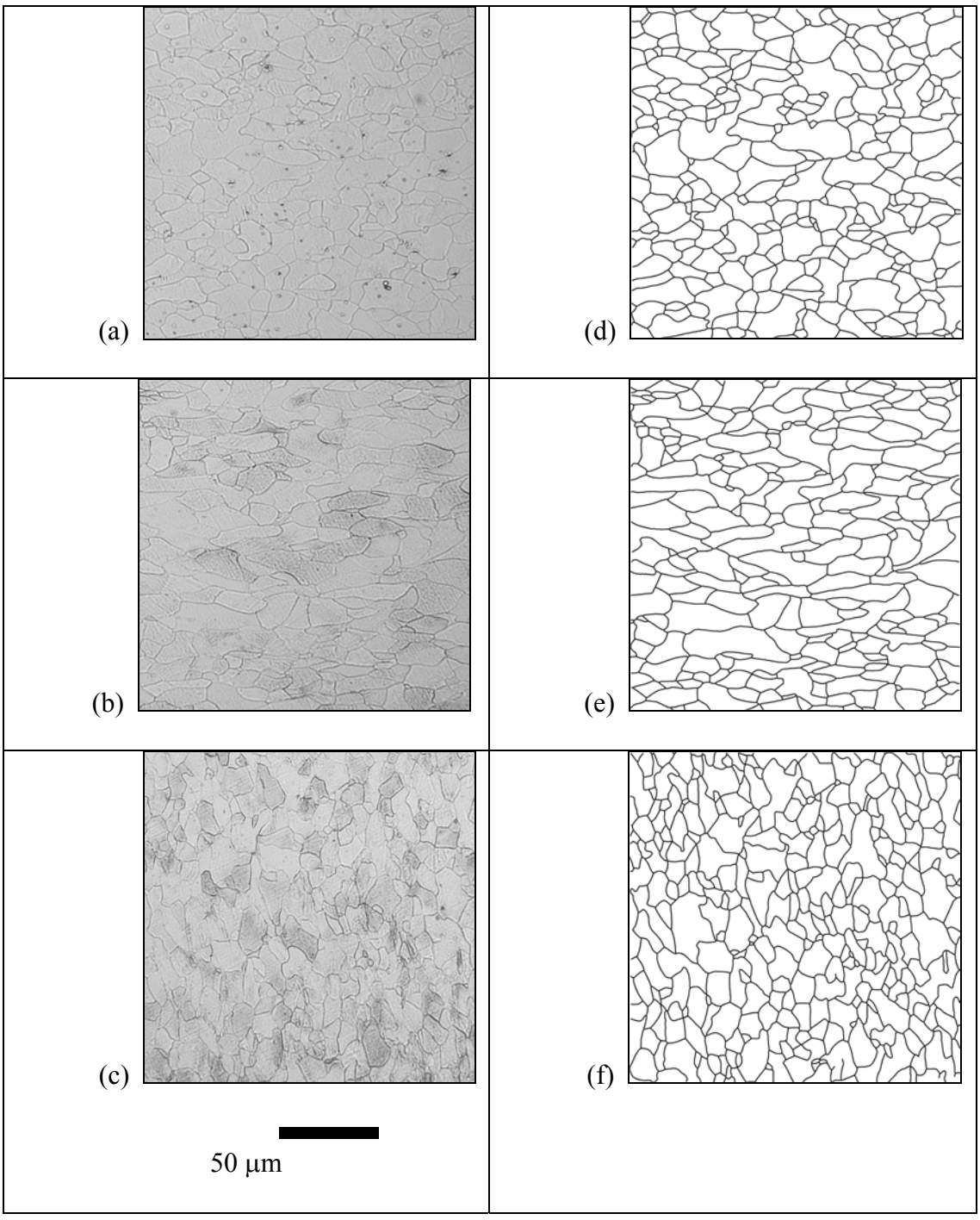
(a)
(d)
(b)
(e)
(c)
(f)
50 μm

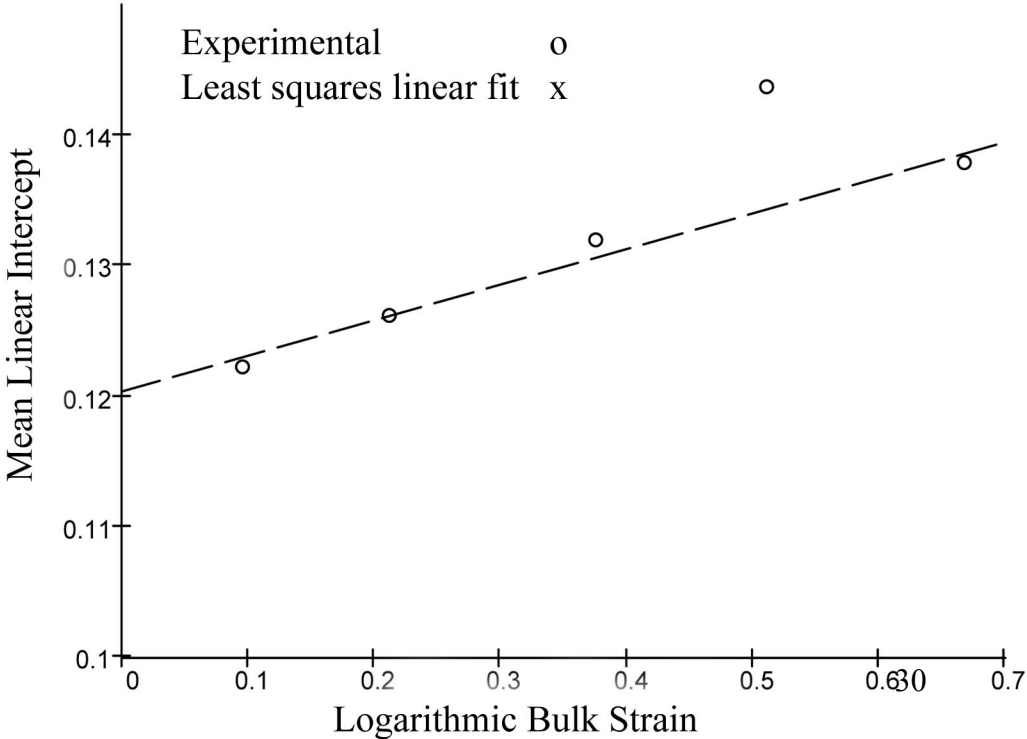
Experimental o
Least squares linear fit x
Mean Linear Intercept
0.14
0.13
0.12
0.11
0.1
0
0.1
0.2
0.3
0.4
0.5
0.6
0.7
Logarithmic Bulk Strain

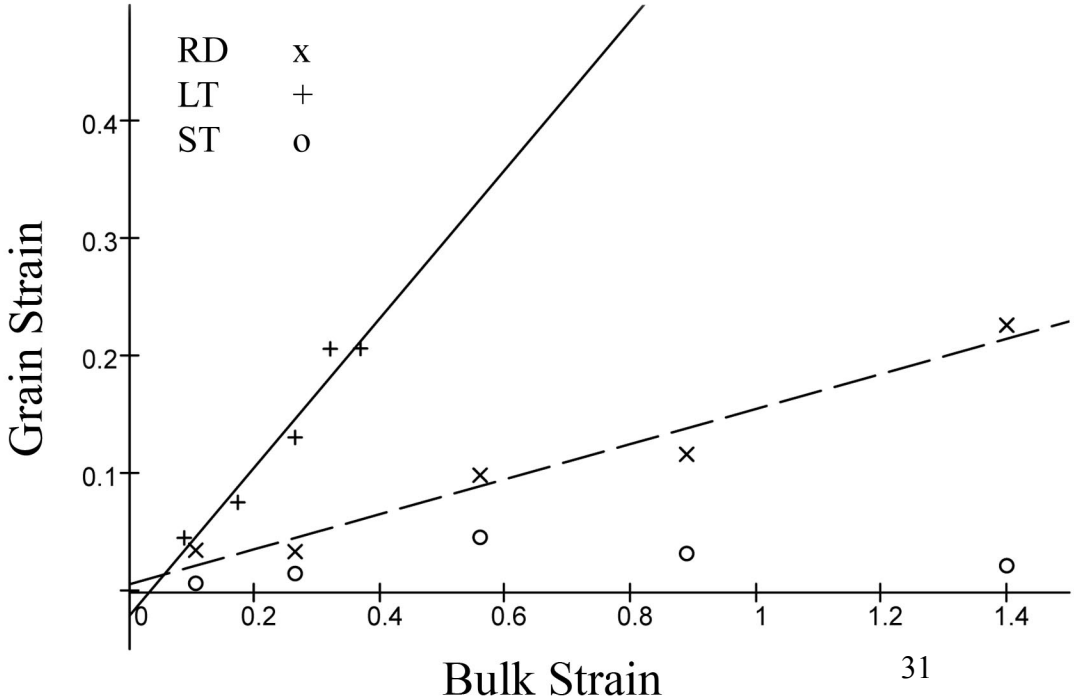
RD x
LT +
ST o
Grain Strain
0.4
0.3
0.2
0.1
0
0.2
0.4
0.6
0.8
1
1.2
1.4
Bulk Strain

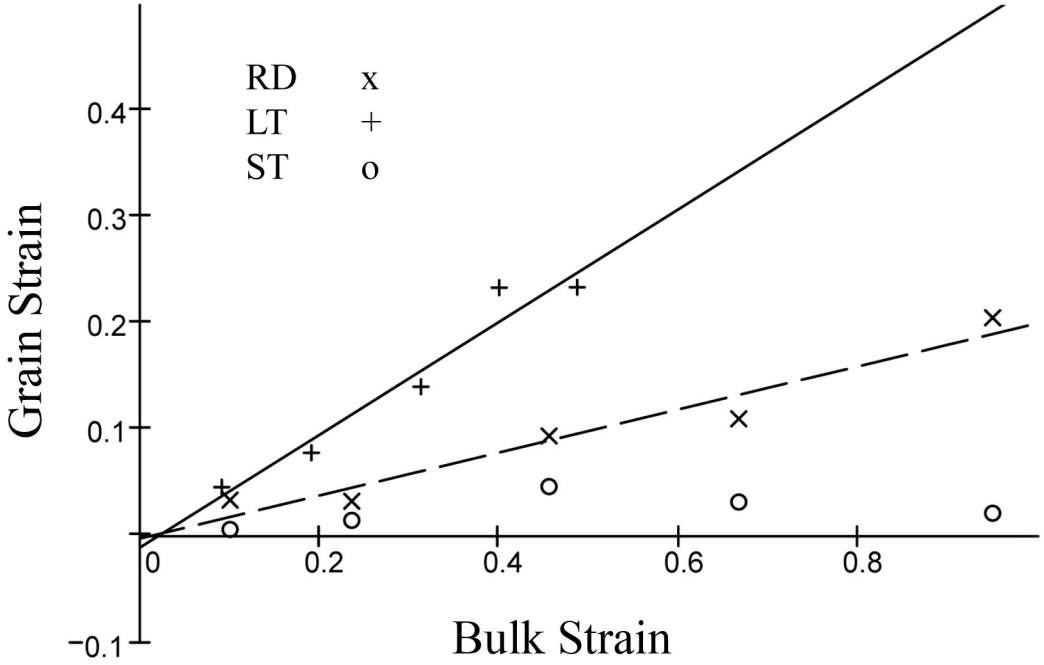
RD x
LT +
ST o
Grain Strain
0.4
0.3
0.2
0.1
−0.1
0
0.2
0.4
0.6
0.8
Bulk Strain

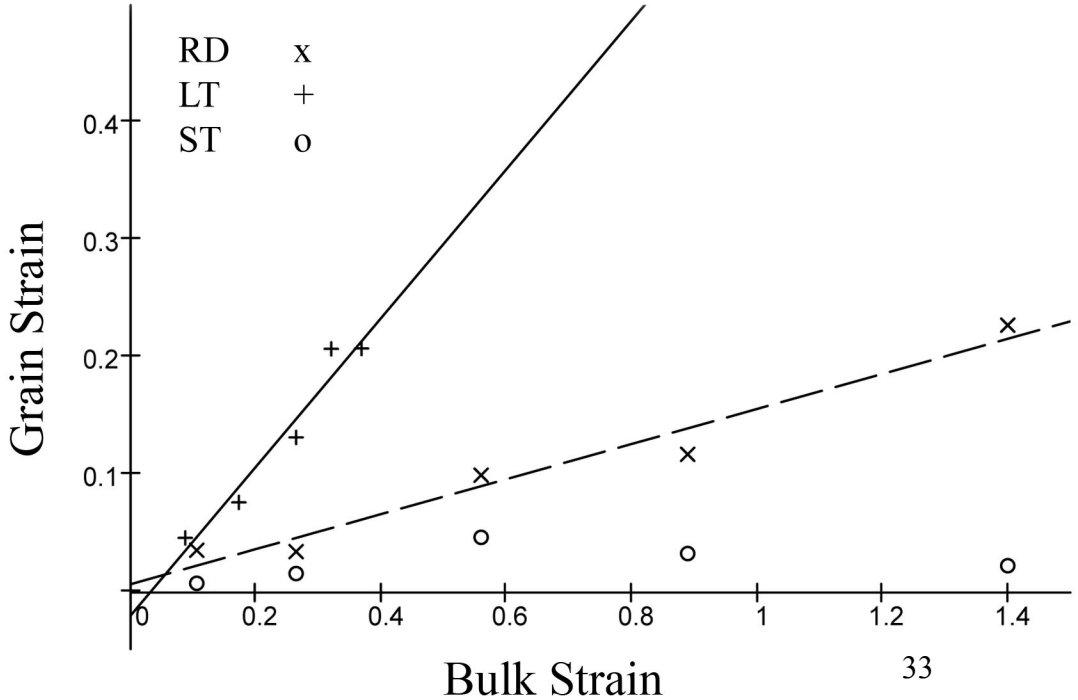
RD x
LT +
ST o
Grain Strain
0.4
0.3
0.2
0.1
0
0.2
0.4
0.6
0.8
1
1.2
1.4
Bulk Strain

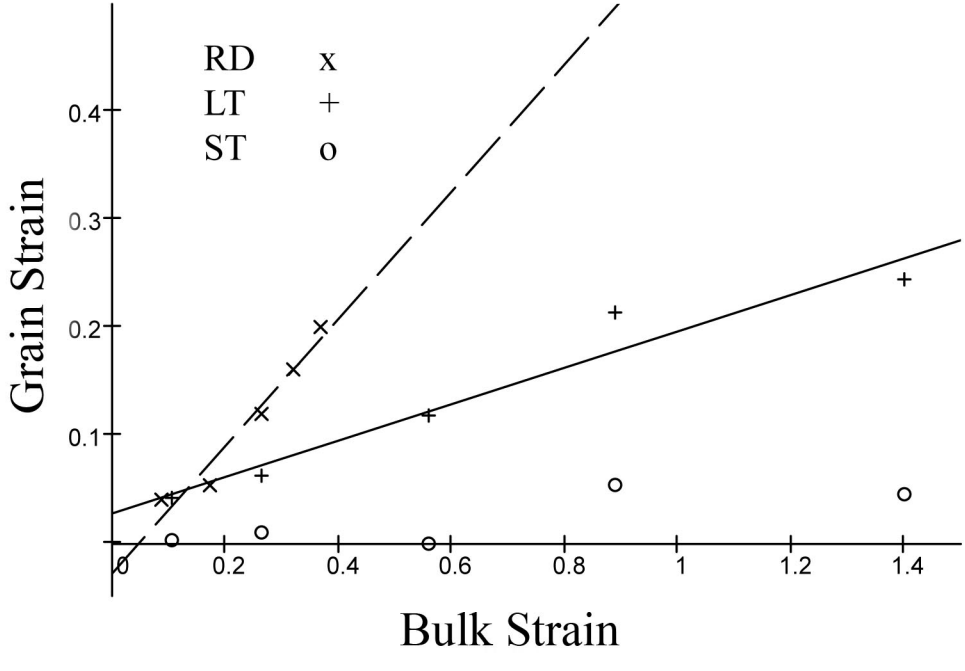
RD x
LT +
ST o
Grain Strain
0.4
0.3
0.2
0.1
0
0.2
0.4
0.6
0.8
1
1.2
1.4
Bulk Strain

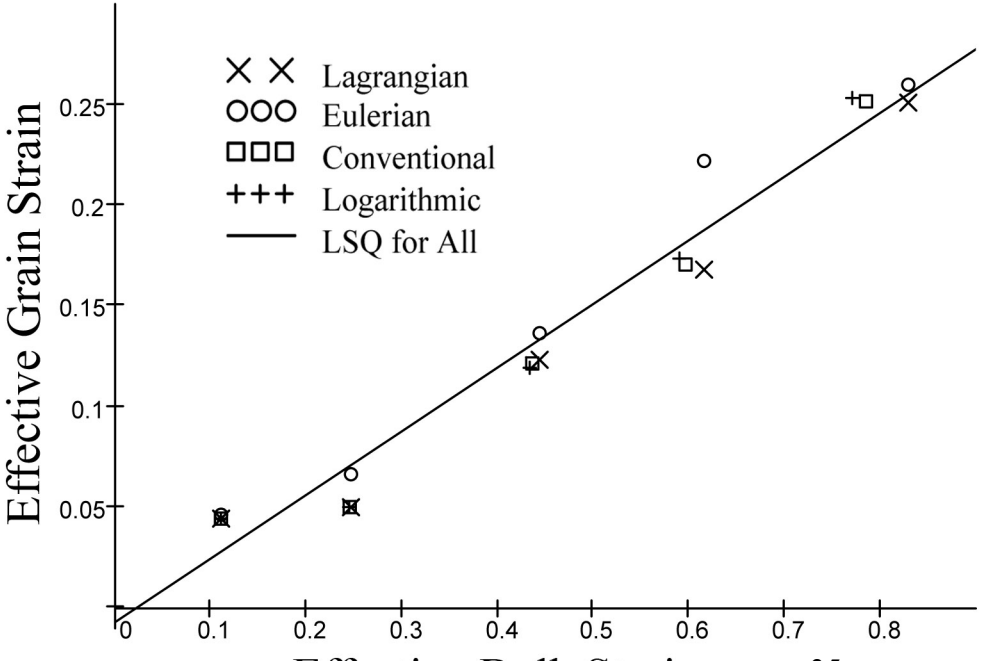
Lagrangian
Eulerian
Conventional
Logarithmic
LSQ for All
Effective Grain Strain
Effective Bulk Strain
0.25
0.2
0.15
0.1
0.05
0
0.1
0.2
0.3
0.4
0.5
0.6
0.7
0.8